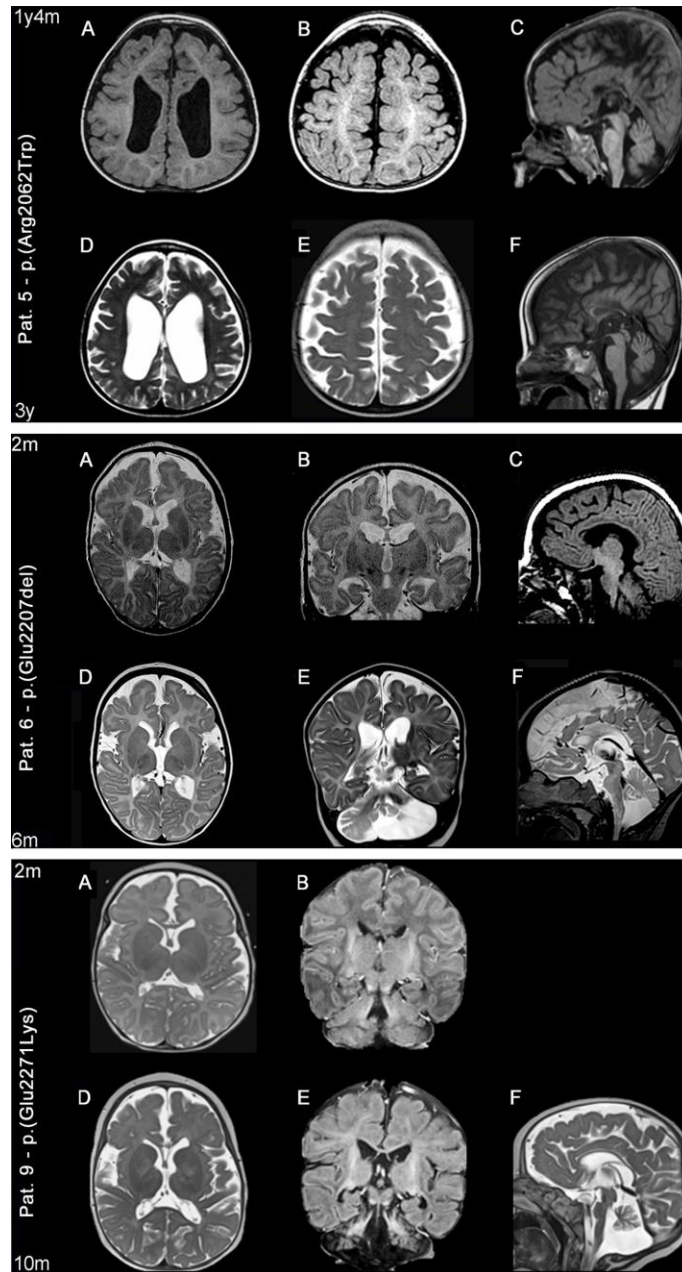
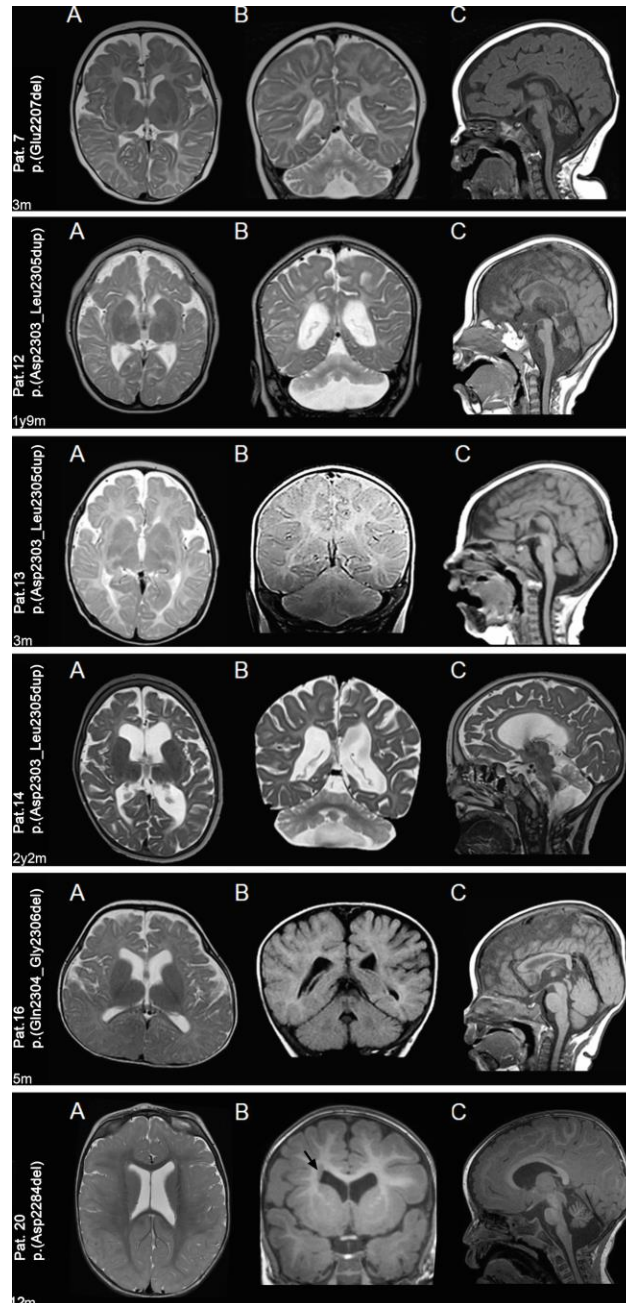


Supplementary Figure 1



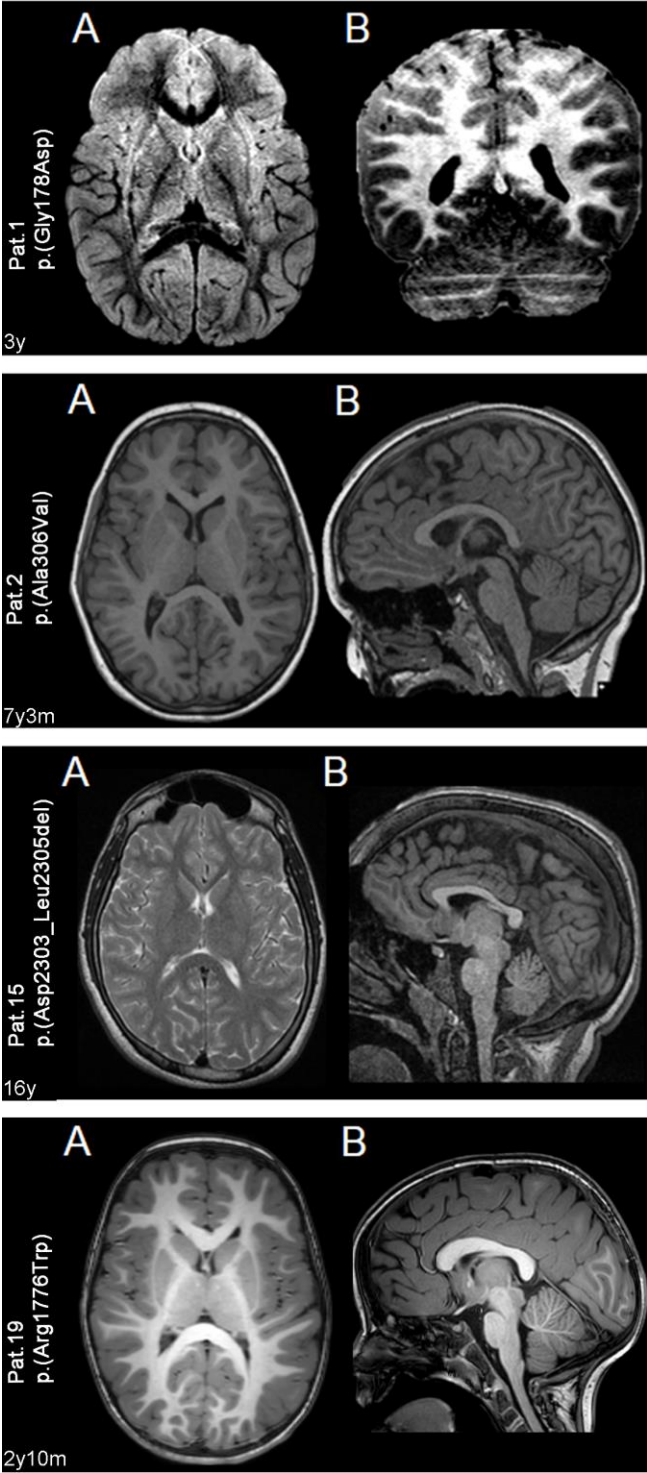
Supplementary Fig. 1: Progression of structural MRI abnormalities in three additional patients who were imaged at least twice during follow-up (#5, 6 and 9) not included in Figure 2. For each patient two sets of comparative axial (A and D), coronal (B and E) and sagittal (C and F) images are presented, taken respectively from the initial and follow-up investigations. Images are at 1.5 to 3T and include T1-W, T2-W and FLAIR sequences. For Patient 9 the initial sagittal image is missing. As also shown in Figure 2, structural abnormalities include a combination of cerebellar and brainstem atrophy, dilated ventricles and subarachnoid spaces, thinning of the corpus callosum and hypomyelination that are variably distributed. Here, however, comparison of initial and follow-up images demonstrates different rates of progression from one patient to another and from one involved structure to another. y: years; m: months.

Supplementary Figure 2



Supplementary Fig. 2: Magnetic resonance imaging characteristics in five patients with *SPTAN1* mutations (#7, 12, 13, 14, 16 and 20). All these patients had only one MRI scan. For each patient a set of axial (A), coronal (B) and sagittal (C) images is shown. Images are at 1.5 to 3T. All images are T2-weighted (W), except images B for Patient 16, 20 and C for Patients 7, 12, 13, 16, and 20. Structural abnormalities include mildly to severely dilated subarachnoid spaces in all patients, cerebellar atrophy with thinning of the brainstem structures of variable severity in Patients 7, 12, and 14, dilated ventricles in Patients 12, 14, 16 and 20, thinning of the corpus callosum in Patients 7, 12-14 and 16, as well as one single periventricular heterotopia in patient 20. Patients 12 and 14 also exhibit severely delayed myelination. y: years; m: months.

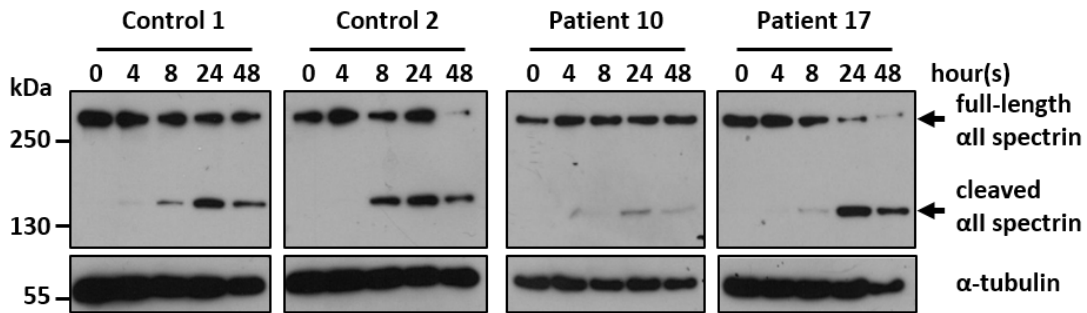
Supplementary Figure 3



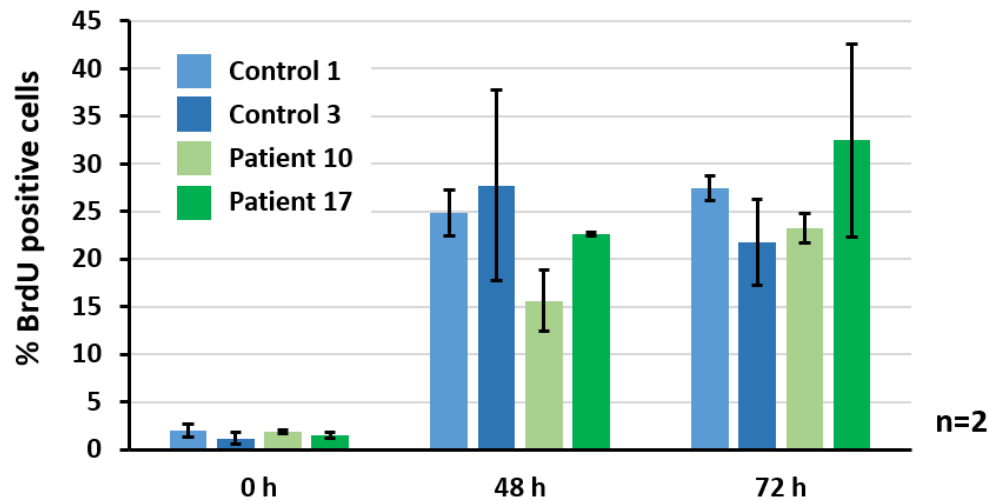
Supplementary Fig. 3: Magnetic resonance images of four patients with *SPTAN1* mutations in whom no structural abnormality is seen (#1, 2, 15 and 19). All these patients had only one MRI scan. Patient 1: A: Axial FLAIR, B: Coronal IR; Patient 2: A: Axial T1, B: Sagittal T1; Patient 15: A: Axial T2, B: Sagittal T1; Patient 19: A: Axial T1, B: Sagittal T1. y: years; m: months.

Supplementary Figure 4

A



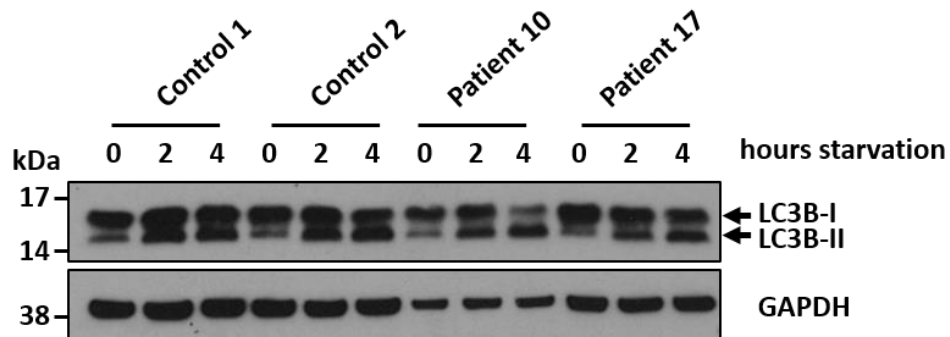
B



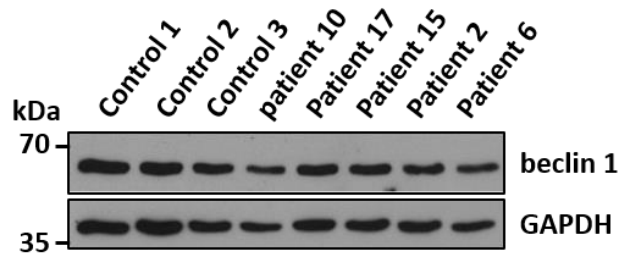
Supplementary Fig. 4: No alteration in apoptotic behavior of fibroblasts harbouring mutations in *SPTAN1* compared with control fibroblasts. (A) No change in the kinetics of α II spectrin cleavage upon staurosporine treatment. Primary fibroblasts of patients 10 and 17 and two control individuals were treated with 1 μ M staurosporine for 0 h, 4 h, 8h, 24 h, and 48 h. Cells were harvested in RIPA buffer, and lysates were subjected to SDS-PAGE and immunoblotting. Representative blots of three independent experiments are shown. (B) Staurosporine-induced apoptosis is not altered in fibroblasts of patients 10 and 17. Cells were treated with 1 μ M staurosporine for 0 h, 48 h, and 72 h. Subsequently, APO-BrdU™ TUNEL assay was performed according to the manufacturer's instructions, and cells were analyzed by flow cytometry. The percentage of BrdU positive cells (mean \pm s.d.) of two (n=2) independent experiments is depicted.

Supplementary Figure 5

A

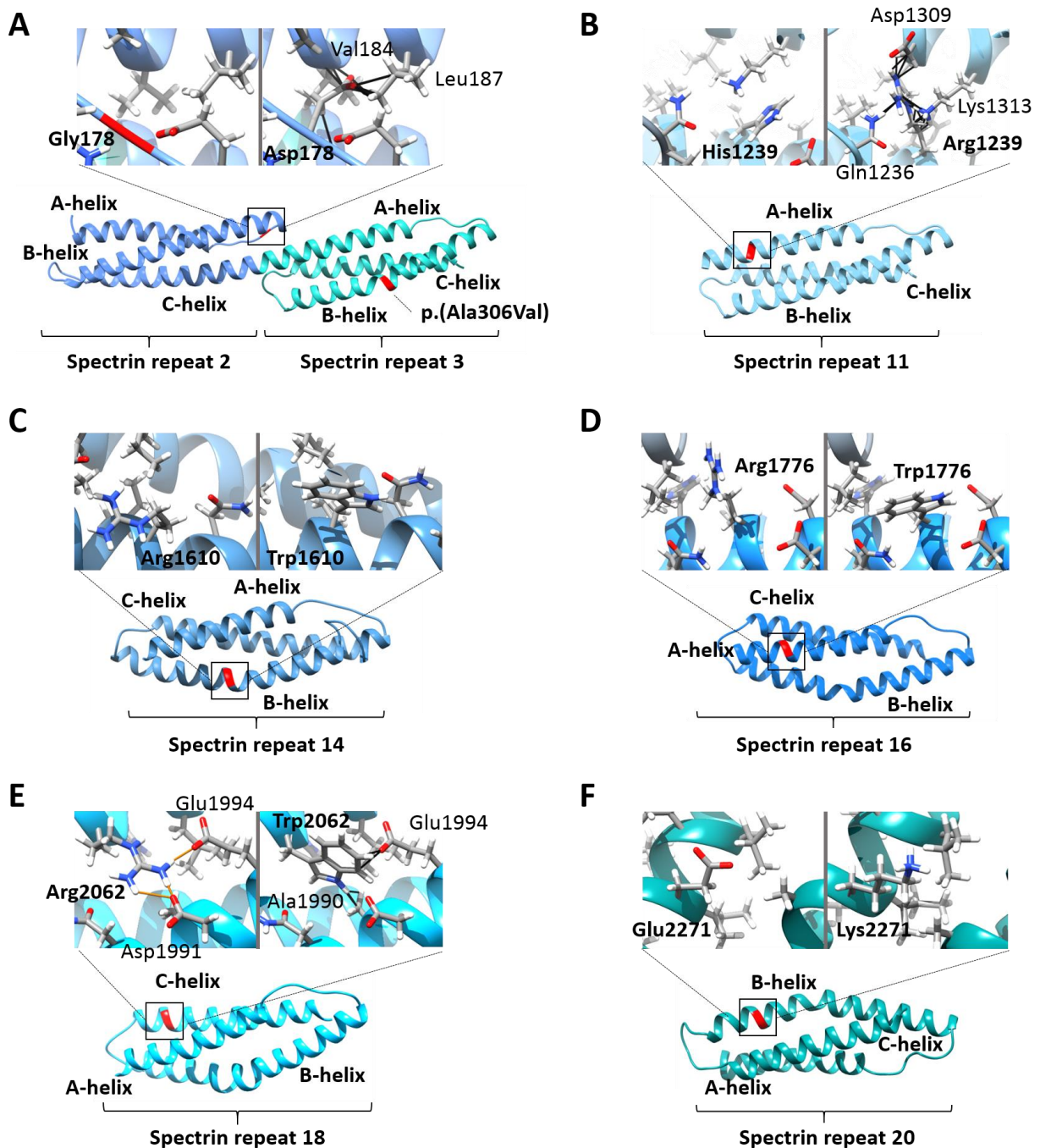


B



Supplementary Fig. 5: No evidence of impaired autophagy in fibroblasts of patients with different *SPTAN1* mutations. (A) Fibroblasts of patients 10 and 17 and two control individuals were cultured in starvation medium (DMEM + 1% FBS) for 0 h, 2 h, and 4 h. Cells were harvested in RIPA buffer, and lysates were subjected to SDS-PAGE and immunoblotting. Upon starvation, the amount of LC3B-II increased similarly over time for all tested fibroblasts. Representative blots of three independent experiments are shown. (B) No difference in the protein amount of the autophagy marker beclin 1 in untreated fibroblasts of five patients (#2, 6, 10, 15 and 17) and control individuals. Cells were harvested, and lysates were subjected to SDS-PAGE and immunoblotting. Representative blots of four independent experiments are shown.

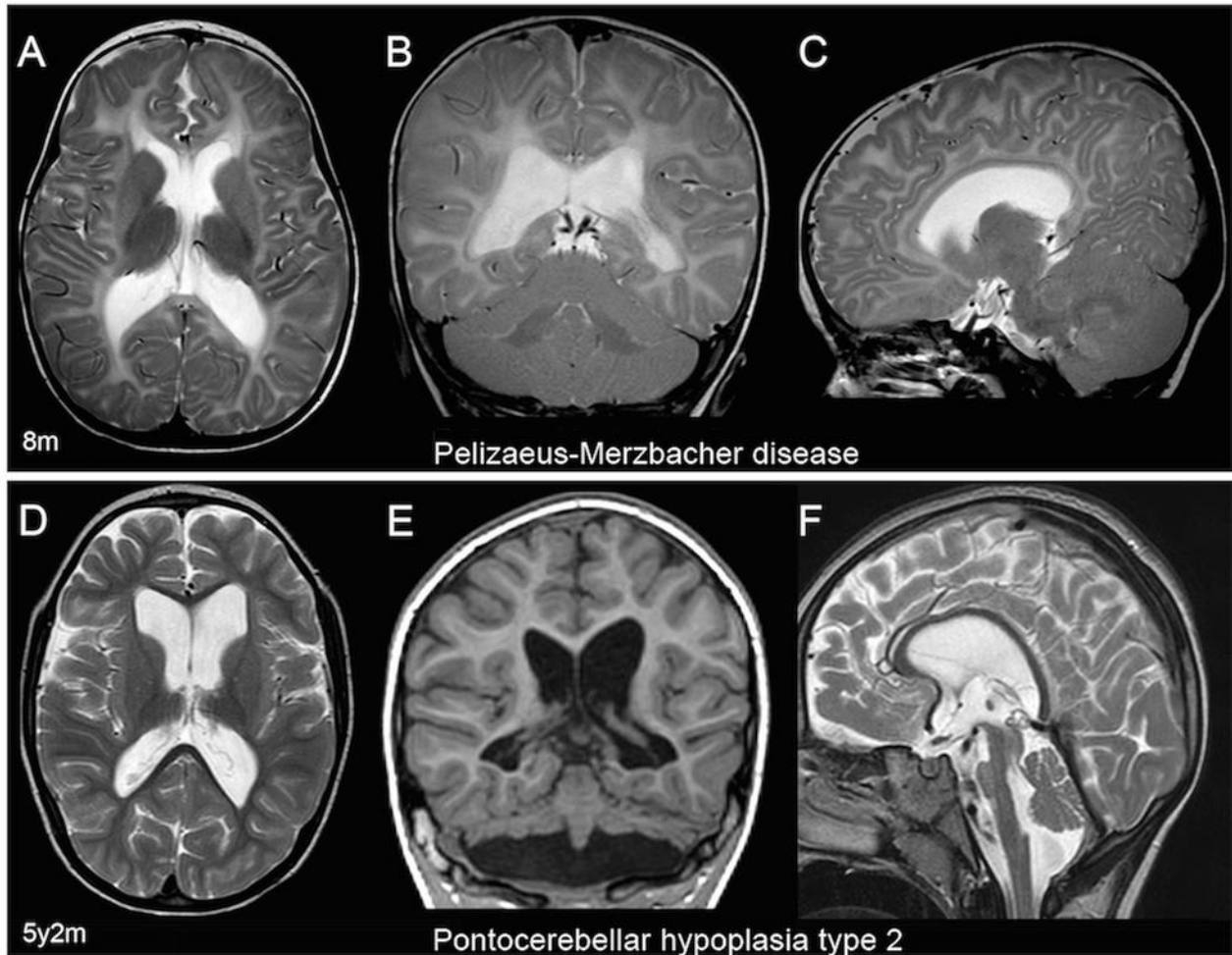
Supplementary Figure 6



Supplementary Fig. 6: Structural impact of *SPTAN1* missense variants. Models of spectrin repeats are shown in blue or turquoise ribbon representations, and the repeat number is indicated; A-, B-, and C-helices are indicated. The position of each disease-associated mutation is highlighted in red within the spectrin repeat. In the panels above the spectrin repeat(s), the wild-type (left) and mutated (right) amino acid and their surroundings are shown in close-ups. Affected residues and neighboring residues within a 5.0-Å range are shown as sticks and side chains are colored by element (carbon = grey, oxygen = red, nitrogen = blue, hydrogen = white). Steric clashes and salt bridges as identified by UCSF Chimera built-in

tools are represented by black and orange lines, respectively. Major interactions of affected residues are shown in (A-F). (A) Gly178 is located within the linker region between the A- and B-helix of spectrin repeat 2 (overview and left panel). Simulation of the missense mutation p.Gly178Asp indicates steric clashes of Asp178 with the main chain of Leu177 (side chain not shown) within the linker region and the main chain of Val184 and the side chain of Leu187 of the B-helix (right panel) probably causing larger steric alterations within spectrin repeat 2. p.(Ala306Val) is located in the B-helix of spectrin repeat 3 (overview). No major steric contacts are predicted for this amino acid change (no close-up shown). (B) Histidine at position 1239 is located within the A-helix of spectrin repeat 11. The change of histidine to arginine is predicted to cause steric clashes with Gln1236 in the A-helix and with Asp1309 and Lys1313 in the C-helix (right panel). (C) The missense variant p.Arg1610Trp affects a highly conserved residue within the B-helix of spectrin repeat 14 (overview and left panel). Simulation of the mutated residue indicates steric clashes for most of the possible sidechain torsions (not shown) except the one which is shown in the close-up (right panel). (D) Arg1776 is located in the A-helix of spectrin repeat 16. Tryptophan at position 1776 can be inserted into the structure without causing steric clashes with neighboring residues (right panel). (E) Arg2062 forms salt bridges with Asp1991 and Glu1994 (left panel). Through the change of Arg2062 to tryptophan within the C-helix of spectrin repeat 18 these salt bridges are disrupted. Instead, steric clashes of tryptophan with the side chains of Ala1990 and Glu1994 of the A-helix (right panel) are observed indicating larger structural alterations. (F) Substitution of Glu2271 by lysine in the B-helix of spectrin repeat 20 is predicted to be tolerated. However, heterodimerisation with β spectrins, which is mediated by α spectrin repeats 19-20 might be impaired due to the p.Glu2271Lys mutation.

Supplementary Figure 7



Supplementary Fig. 7: Representative T2 (A, B, C, D, F) and T1 (E) weighted MR images of two patients with genetically proven Pelizaeus-Merzbacher disease (A-C; *PLP1* gene duplication) and pontocerebellar hypoplasia type 2 (PCH2) (D-F: *TSEN54* mutation). At age 8 months, MRI in the patient with Pelizaeus-Merzbacher disease shows high intensity signal in the white matter and ventricular dilatation. These findings may be difficult to differentiate from the hypomyelination observed in most infants with *SPTAN1* mutations, in which, however, early atrophic brainstem and cerebellar changes are usually present. The atrophic brainstem, pons and cerebellum, associated with thin corpus callosum and dilated ventricles in the patient with PCH2 are very similar to MR findings observed in children with *SPTAN1* mutations. y: years; m: months.

Supplementary Table 1

| Patient | Inheritance | Reference | Nucleotide change | Amino acid change | Phenotype (Age at last follow-up) |
|---------|----------------|-------------------------------------|-------------------|-------------------------------------|--|
| 1 | n.a. | (Gilissen <i>et al.</i> , 2014) | c.271G>A | p.(Glu91Lys) | ID (n.a.) |
| 2 | paternal | (An <i>et al.</i> , 2014) | c.362G>T | p.(Arg121Lys) | ASD (n.a.) |
| 3 | <i>de novo</i> | (Hamdan <i>et al.</i> , 2012) | c.1697G>C | p.(Arg566Pro) | ID (no Sz) (9 y) |
| 4 | n.a. | (Retterer <i>et al.</i> , 2016) | c.6103C>T | p.(Gln2035*) ^a | Abnormality of the nervous system (n.a.) |
| 5 | <i>de novo</i> | (Yavarna <i>et al.</i> , 2015) | c.6103C>T | p.(Gln2035*) ^a | Sz, microcephaly, ACC, cerebellar hypoplasia (n.a.) |
| 6 | <i>de novo</i> | (Hamdan <i>et al.</i> , 2012) | c.6605_6607del | p.(Gln2202del) | severe ID, generalized epilepsy, severe atrophy of the cerebellum and mild atrophy of the brainstem (11 y) |
| 7 | <i>de novo</i> | (Saitsu <i>et al.</i> , 2010) | c.6619_6621del | p.(Glu2207del) ^a | EIEE5 (11 y) |
| 8 | <i>de novo</i> | (Writzl <i>et al.</i> , 2012) | c.6619_6621del | p.(Glu2207del) ^a | EIEE5, coloboma-like optic disc (3 y) |
| 9 | <i>de novo</i> | (Nonoda <i>et al.</i> , 2013) | c.6908_6916dup | p.(Asp2303_Leu2305dup) ^a | EIEE5 (died at 2 y) |
| 10 | <i>de novo</i> | (Tohyama <i>et al.</i> , 2015) | c.6908_6916dup | p.(Asp2303_Leu2305dup) ^a | EIEE5 (2 y) |
| 11 | <i>de novo</i> | (Tohyama <i>et al.</i> , 2015) | c.6908_6916dup | p.(Asp2303_Leu2305dup) ^a | EIEE5 (6 y) |
| 12 | n.a. | (Ream and Mikati, 2014) | c.6910_6918dup | p.(Gln2304_Gly2306dup) | EIEE5 (n.a.) |
| 13 | <i>de novo</i> | (Saitsu <i>et al.</i> , 2010) | c.6923_6928dup | p.(Arg2308_Met2309dup) ^a | EIEE5 (died at 3 y from myocarditis) |
| 14 | <i>de novo</i> | (Stavropoulos <i>et al.</i> , 2016) | c.6947A>C | p.(Gln2316Pro) | Microcephaly, hypotonia and intractable seizures |

Supplementary Table 1: Previously published 14 individuals with alterations in *SPTAN1* (mRNA reference number: NM_001130438). Phenotypic data and information on type of inheritance are given, when available. ^a recurrent mutation, see also this study. ACC – agenesis of corpus callosum, ASD – autism spectrum disorder, EIEE5 – West syndrome with hypomyelination, pontocerebellar atrophy and absence of visual attention, ID – intellectual disability, n.a. – not available, Sz – Seizures, y – years.

Supplementary Table 2

| Patient(s) | Nucleotide change | Amino acid change | α spectrin repeat | CADD | REVEL | ACMG Criteria | ACMG |
|------------|---|------------------------|--------------------------------|-------|-------|-----------------------------------|------|
| 1 | c.533G>A | p.(Gly178Asp) | 2 | 32 | 0.644 | PM2, PM6, PP2, PP3 | LP |
| 2 | c.917C>T | p.(Ala306Val) | 3 | 25.7 | 0.204 | PM2, PM6, PP2, PP3 | LP |
| 3 | c.3716A>G | p.(His1239Arg) | 11 | 24.1 | 0.610 | PM2, PM6, PP2, PP3 | LP |
| 4 | c.4828C>T | p.(Arg1610Trp) | 14 | 35 | 0.303 | PM2, PM6, PP2, PP3 | LP |
| 19 | c.5326C>T | p.(Arg1776Trp) | 16 | 35 | 0.440 | PM2, PM6, PP2, PP3 | LP |
| 5 | c.6184C>T | p.(Arg2062Trp) | 18 | 35 | 0.532 | PM2, PM6, PP2, PP3 | LP |
| 6 + 7 | c.6619_6621del | p.(Glu2207del) | 19-20 | 18.57 | – | PS3, PS4, PM2, PM4, PM6, PP3 | P |
| 8 | c.6622_6624del | p.(Asn2208del) | 19-20 | 19.22 | – | PM2, PM4, PM6, PP3 | LP |
| 9 | c.6811G>A | p.(Glu2271Lys) | 20 | 27.1 | 0.565 | PM2, PM6, PP2, PP3 | LP |
| 20 | c.6850_6852del | p.(Asp2284del) | 20 | 21.7 | – | PS2, PM2, PM4, PP3 | LP |
| 10+11+12 | c.6908_6916dup | p.(Asp2303_Leu2305dup) | 20 | 19.27 | – | PS2, PS4, PM1, PM2, PM4, PP3 | P |
| 13+14 | c.6907_6915dup | p.(Asp2303_Leu2305dup) | 20 | 18.16 | – | PS1, PM1, PM2, PM4, PM6, PP3 | P |
| 15 | c.6908_6916del | p.(Asp2303_Leu2305del) | 20 | 22.5 | – | PM1, PM2, PM4, PM6, PP3 | LP |
| 16 | c.6910_6918del | p.(Gln2304_Gly2306del) | 20 | 22.6 | – | PS2, PM1, PM2, PM4, PP3 | P |
| 17 | c.6923_6928dup | p.(Arg2308_Met2309dup) | 20 | 20.6 | – | PS3, PS4, PM1, PM2, PM4, PM6, PP3 | P |
| 18 | arr[hg19] 9q34.11(131,349,701- 131,351,531)x1 | p.(Ala927_Lys1002del) | 9 (including SH3 domain) | – | – | PM2, PM4, PM6 | LP |

Suppl
emen
tary
Table
2: *In
silico
path
ogeni
city
predi
ction
of
muta
tions
in
SPTA
N1
(mRN
A
refer
ence*

number: NM_001130438). Localisation of the amino acid alterations within α spectrin repeats is given. The functional impact of the identified variants was predicted by the Combined Annotation Dependent Depletion (CADD) and Rare exome variant ensemble learner (REVEL) scoring systems. CADD is a framework that integrates multiple annotations into one metric by contrasting variants that survived natural selection with simulated mutations. Reported CADD score is a phred-like rank score based upon the rank of that variant's score among all possible single nucleotide variants of hg19, with 10 corresponding to the top 10%, 20 at the top 1%, and 30 at the top 0.1%. The larger the score the more likely the variant has deleterious effects; the score range observed here is strongly supportive of pathogenicity, with all observed variants ranking above ~99% of all variants in a typical genome and scoring similarly to variants reported in ClinVar as pathogenic (~85% of which score >15) (Kircher *et al.*, 2014). REVEL is an ensemble method predicting the pathogenicity of missense variants with a strength for distinguishing pathogenic from rare neutral variants with a score ranging from 0-1. The higher the score the more likely the variant is pathogenic (Ioannidis *et al.*, 2016). Classification of variants was performed according to the guidelines of the American College of Medical Genetics (Richards *et al.*, 2015), predicting all alterations as likely pathogenic (LP) or pathogenic (P).

References

- An JY, Cristino AS, Zhao Q, Edson J, Williams SM, Ravine D, *et al.* Towards a molecular characterization of autism spectrum disorders: an exome sequencing and systems approach. *Translational Psychiatry* 2014; 4.
- Gilissen C, Hehir-Kwa JY, Thung DT, van de Vorst M, van Bon BWM, Willemsen MH, *et al.* Genome sequencing identifies major causes of severe intellectual disability. *Nature* 2014; 511(7509): 344-+.
- Hamdan FF, Saitsu H, Nishiyama K, Gauthier J, Dobrzeniecka S, Spiegelman D, *et al.* Identification of a novel in-frame de novo mutation in SPTAN1 in intellectual disability and pontocerebellar atrophy. *European Journal of Human Genetics* 2012; 20(7): 796-800.
- Ioannidis NM, Rothstein JH, Pejaver V, Middha S, McDonnell SK, Baheti S, *et al.* REVEL: An Ensemble Method for Predicting the Pathogenicity of Rare Missense Variants. *American Journal of Human Genetics* 2016; 99(4): 877-85.
- Kircher M, Witten DM, Jain P, O'Roak BJ, Cooper GM, Shendure J. A general framework for estimating the relative pathogenicity of human genetic variants. *Nature Genetics* 2014; 46(3): 310-+.
- Nonoda Y, Saito Y, Nagai S, Sasaki M, Iwasaki T, Matsumoto N, *et al.* Progressive diffuse brain atrophy in West syndrome with marked hypomyelination due to SPTAN1 gene mutation. *Brain & Development* 2013; 35(3): 280-3.
- Ream MA, Mikati MA. Clinical utility of genetic testing in pediatric drug-resistant epilepsy: A pilot study. *Epilepsy & Behavior* 2014; 37: 241-8.
- Retterer K, Juusola J, Cho MT, Vitazka P, Millan F, Gibellini F, *et al.* Clinical application of whole-exome sequencing across clinical indications. *Genetics in Medicine* 2016; 18(7): 696-704.
- Richards S, Aziz N, Bale S, Bick D, Das S, Gastier-Foster J, *et al.* Standards and guidelines for the interpretation of sequence variants: a joint consensus recommendation of the American College of Medical Genetics and Genomics and the Association for Molecular Pathology. *Genetics in Medicine* 2015; 17(5): 405-24.
- Saitsu H, Tohyama J, Kumada T, Egawa K, Hamada K, Okada I, *et al.* Dominant-Negative Mutations in alpha-II Spectrin Cause West Syndrome with Severe Cerebral Hypomyelination, Spastic Quadriplegia, and Developmental Delay. *American Journal of Human Genetics* 2010; 86(6): 881-91.
- Stavropoulos DJ, Merico D, Jobling R, Bowdin S, Monfared N, Thiruvahindrapuram B, *et al.* Whole-genome sequencing expands diagnostic utility and improves clinical management in paediatric medicine. *Npj Genomic Medicine* 2016; 1: 15012.
- Tohyama J, Nakashima M, Nabatame S, Gaik-Siew C, Miyata R, Renner-Primec Z, *et al.* SPTAN1 encephalopathy: distinct phenotypes and genotypes. *Journal of Human Genetics* 2015; 60(4): 167-73.
- Writzl K, Primec ZR, Strazisar BG, Osredkar D, Pecaric-Meglic N, Kranjc BS, *et al.* Early onset West syndrome with severe hypomyelination and coloboma-like optic discs in a girl with SPTAN1 mutation. *Epilepsia* 2012; 53(6): e106-e110.
- Yavarna T, Al-Dewik N, Al-Mureikhi M, Ali R, Al-Mesaifri F, Mahmoud L, *et al.* High diagnostic yield of clinical exome sequencing in Middle Eastern patients with Mendelian disorders. *Human Genetics* 2015; 134(9): 967-80.